A Spectroscopic System for High-Speed Inspection of Poultry Carcasses

K. Chao, Y. R. Chen, D. E. Chan

Abstract. *A visible/near−infrared spectroscopic system for high−speed on−line poultry carcass inspection was developed and demonstrated. The inspection system, which was an area scanning system designed to measure the interactance spectra of poultry carcasses in the visible to near−infrared regions, consisted of a fiber−optic probe, a spectrograph, a spectroscopic charge coupled device detector, a quartz tungsten halogen light source, an industrial computer, and in−house developed software modules. On−line trials of the visible/near−infrared chicken inspection system were conducted during a 5−day period in a poultry processing plant in Athens, Georgia. Spectra (431 to 943 nm) of 450 wholesome and 426 unwholesome chicken carcasses were measured. The instrument measured the spectra of veterinarian−selected carcasses on a processing line running at speeds of 140 and 180 birds/min. Results showed this visible/near−infrared system can be used to differentiate between wholesome and unwholesome poultry carcasses at high speeds. For the 140−bird/min line speed, the best model achieved classification accuracies of 95% for wholesome and 92% for unwholesome birds. For the 180−bird/min line speed, the best model achieved classification accuracies of 94% and 92% for wholesome and unwholesome birds, respectively. The system is ready to be implemented for operation on high−speed poultry processing lines.*

Keywords. *Automation, Food safety, Poultry inspection, Modeling, Visible/near−infrared spectroscopy.*

Automatic processing systems are needed in the poultry industry to improve product safety, quality, consistency, and increase processing efficiency by increasing line throughputs and reducing wastewater output. One of the most important aspects of automation in poultry processing systems is the inspection of poultry carcasses. Currently, each chicken intended for sale to U.S. consumers is required by law to be inspected post−mortem by a USDA/FSIS (United States Department of Agriculture/Food Safety and Inspection Service) inspector for its wholesomeness (USDA, 1984). These inspectors visually examine the exterior, the inner surfaces of the body cavity, and the organs of each carcass for indications of diseases or defects. For effective inspection and occupational considerations, each inspector is limited to a maximum of 35 birds/min. This current inspection system limits the production efficiency of processing plants that are seeking to satisfy increasing consumer demand for poultry products. One possible solution to this problem is for poultry processing plants to install on−line instrumental inspection systems that can accurately screen for wholesome carcasses. Inspectors then would only have to "re−inspect" questionable carcasses to insure that wholesome carcasses are not discarded. This approach would dramatically reduce the number of birds requiring human inspection. An obvious benefit of automatic poultry inspection would be improved overall production efficiency of the processing plants.

Most poultry processing plants in the United States currently use one of two evisceration configurations, either a Stream−line Inspection System (SIS) or a New Efficient Line Speed (NELS) system. Under SIS, an Evisceration Line operates at 70 shackles/min with two USDA inspection stations on it. A NELS Evisceration Line runs at 91 shackles/min with three USDA inspection stations. At each inspection station, the USDA inspector works with the aid of a helper and a trimmer. Figure 1 shows the typical layout of a poultry slaughter system with one Kill Line feeding two Evisceration Lines. On the Kill Line, birds are stunned, bled, scalded, and defeathered, and heads and paws are removed, before rehanging onto the Evisceration Line. Developing an automated inspection system for operation on the Kill Line presents two major benefits. First, with a single rejection point on the Kill Line, no condemnable birds would enter the Evisceration Line, allowing for better hygiene, no empty shackles, and higher line speed on the Evisceration Line. Second, working with known technology to remove rejected birds from the Kill Line, such a system would be easily integrated into product−tracking systems. To operate on the Kill Line, any automated inspection system must be able to function at the high speeds of the Kill Line, currently at 140 or 180 birds per minute (bpm).

Two major conditions can cause a carcass to be removed from the processing line (USDA, 1998). The first is an infectious condition, such as septicemia/toxemia. Septicemia/toxemia is a systemic disease caused by pathogenic

Article was submitted for review in August 2003; approved for publication by the Food & Process Engineering Institute Division of ASAE in March 2004.

Mention of trade names or commercial products is solely for the purpose of providing specific information and does not imply endorsement or recommendation by the USDA.

The authors are **Kuanglin Chao, ASAE Member,** Research Scientist, **Yud−Ren Chen, ASAE Member Engineer,** Research Leader, **Diane Chan,** Agricultural Engineer; USDA/ARS/ISL, Beltsville, Maryland. **Corresponding author:** Kuanglin Chao, USDA/ARS/ISL, Building 303, BARC−East, 10300 Baltimore Avenue, Beltsville, MD 20705−2350; phone: 301−504−8450; fax: 301−504−9466; e−mail: chaok@ba.ars.usda.gov.

  ISSN 0883−8542

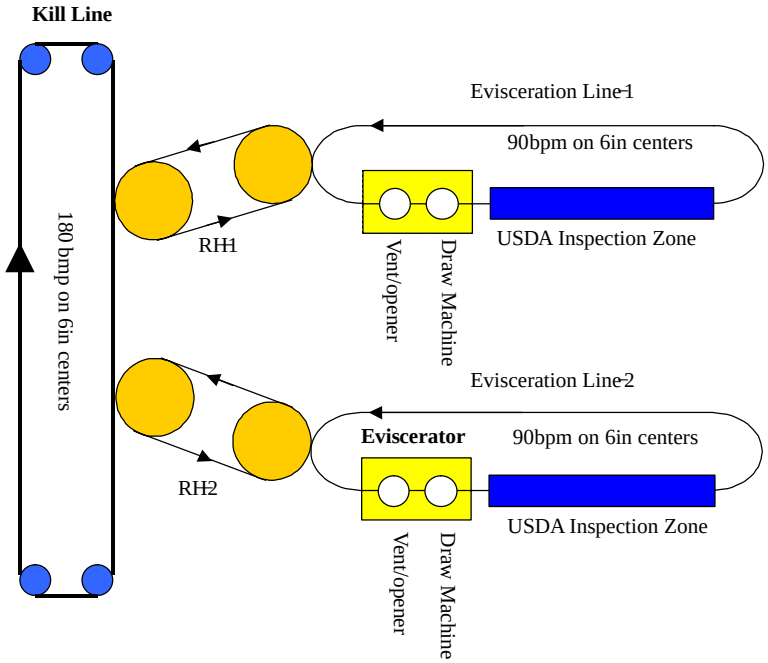

Figure 1. Poultry processing line layout. RH = rehanger; bpm = birds per minute.

microorganisms in the blood, and such carcasses often show dark red skin discolorations. The second type is Avian Disease, which includes leukosis complex, airsacculitis, ascites, cadaver, and inflammatory process (IP), among others. Airsacculitis is inflammation of the air sacs. Ascites is characterized by excess fluid in the air sacs and body cavities. Improper slaughter cuts or inadequate bleeding time can result in Cadaver carcasses. Systemic conditions, or localized conditions with systemic symptoms, require condemnation of entire carcasses. However, carcasses showing localized conditions without systemic symptoms can be further reprocessed, such as vacuum removal of excess fluid in the body cavities or portioning of carcass parts.

Spectral imaging techniques have been shown to be useful for detecting surface discolorations and contaminations for automated poultry carcass inspection (Daley et al., 1994; Park et al., 1996; Lawrence et al., 2002; Chao et al., 2002). Visible/Near−Infrared (Vis/NIR) spectroscopy has been shown capable of detecting systemic conditions manifesting in skin and tissue changes. A Vis/NIR spectroscopy technique was first used to classify wholesome and unwholesome carcasses by Chen and Massie (1993). Optimal wavelengths for correlating the spectral reflectance and interactance with the condition of the poultry carcasses were obtained. They concluded that this technique can be used to separate wholesome carcasses from the unwholesome carcasses with a classification accuracy of 93% for wholesome carcasses and 96% for the unwholesome carcasses.

A Vis/NIR spectroscopic (471 to 964 nm) system was used for classifying poultry carcasses on−site at a slaughter plant (Chen et al., 1996). Fresh carcasses were taken off−line, and the Vis/NIR probe was placed in direct contact with each sample for a stationary reflectance measurement of about 2 s. Classification of poultry carcasses into wholesome, septicemia/toxemia, and cadaver classes were achieved with an average accuracy of 93%.

A transportable photodiode array spectroscopic system was then developed, and on−line trials were performed during an 8−day period in a chicken processing plant in New Holland, Pennsylvania (Chen et al., 2000). Spectra (470 to 960 nm) of 1750 (1174 wholesome and 576 unwholesome) chicken carcasses were measured. The instrument measured the spectra of veterinarian−selected carcasses running on a processing line at 70 bpm. The detection time was 300 ms. Classification models, using principal component analysis as a data pretreatment for input into neural networks, were able to classify the carcasses with a success rate of 95%. The results showed promise for using a Vis/NIR spectroscopic system to separate unwholesome from wholesome carcasses on−line in a poultry−processing environment.

Based on previous studies, a new transportable Vis/NIR spectroscopic system with improved data acquisition, processing, and modeling functionality was developed in order to operate on high−speed processing lines. This article reports on the results of testing this system at a commercial poultry processing facility.

Materials and Methods

Chicken Samples

Broilers were processed at a commercial poultry processing plant in Athens, Georgia. Chicken carcasses from the evisceration line were identified as “wholesome and passed” or “unwholesome” by FSIS inspectors on−site. The unwholesome chicken carcasses were identified according to the FSIS condemnation disposition criteria (i.e., exhibit signs of systemic conditions) that may render the carcass and its parts adulterated. A total of 426−unwholesome carcasses (92 septicemia, 256 airsacculitis, 57 ascites, 21 IP) and 450−inspected and passed wholesome carcasses were collected over a 5−day period in May of 2003.

POULTRY INSPECTION SYSTEM

The ISL poultry inspection system is an area (poultry carcass) scanning system designed to measure the interactance spectra of poultry carcasses in the VIS to NIR regions. The poultry inspection system consisted of a fiber−optic probe, a spectrograph, a spectroscopic CCD (Charge Coupled Device) detector, a quartz tungsten halogen light source, an industrial computer, and in−house developed software modules.

Equipment

A bifurcated fiber−optic probe (Schott−Fostec, Auburn, N.Y.) was designed and fabricated to measure light reflectance in poultry carcass. The probe, as shown in figure 2, consisted of inner and outer fiber−optic bundles. Fibers of the outer optic bundles transmitted light to the chicken carcass, and fibers of the inner optic bundle returned reflected light to a photo detector. The outer bundles were angled 10 degrees inward, providing a minimum working distance of approximately 2 cm with a 200−mm^2 illuminated spot (approximately 16 mm diameter). Light from a 100−W quartz tungsten halogen light bulb was focused on the light source circular end of the outer optical bundles with the use of a condensing/imaging lens assembly (*f*/1.8, 33−mm aperture, UV−grade fused silica). This light energy traveled though the fiber−optic cable and exited by means of the concentric ring of outer optical bundles to illuminate samples. After interacting with the chicken sample, the light energy was then collected through the central 7.5−mm diameter aperture. Transmitted through the inner optic fiber, the light exited through a 4−mm high × 50−µm wide slit. The spectrograph (MS125, Oriel Instruments, Stratford, Conn.) had a focal length of 120 mm and a grating ruling of 400 lines/mm. The fixed entrance slit of the spectrograph was 3 mm high × 10 µm wide. Light reflectance was measured using a 1024− × 128− (pixel size of 26 µm^2) CCD detector (Oriel model 78440). The CCD detector was thermoelectrically cooled, front illuminated with UV coating, and had a spectral response from 180 to 1000 nm with a maximum readout time of 300 spectra/s with a 1024−pixel array (full vertical binning). The CCD detector was connected to an analog to digital conversion board (Oriel model CCI−001) installed in an industrial computer.

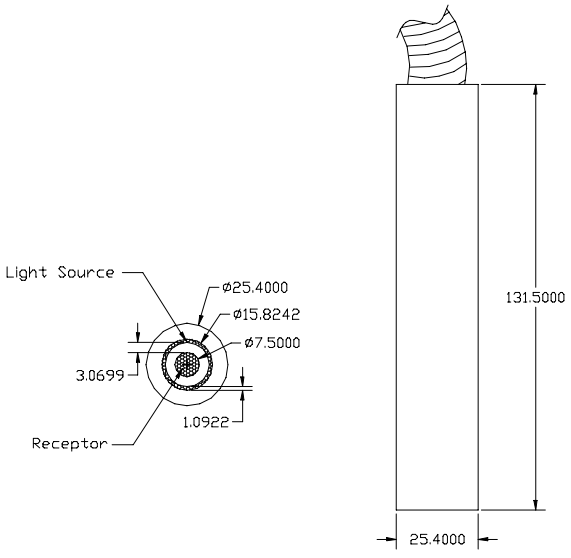

Figure 2. Schematic of the bifurcated fiber−optic probe (all dimensions in mm).

Software Modules

The Automated Poultry Inspector (API) software was developed to integrate hardware components for automated poultry carcass inspection. The LabView (National Instruments, Austin, Tex.) programming language was utilized to develop the API software. The front panel of the API, shown in figure 3, consisted of four primary functions: system initialization, data collection, data analysis and modeling, and prediction of poultry carcasses.

The system initialization module utilized the 32−bit driver (ATMCD32D.DLL, Oriel Instruments, Stratford, Conn.) to initialize the CCD detector and set CCD temperature control, data acquisition mode, exposure time, and data readout mode. After system initialization, the data collection module enabled real−time data acquisition and data storage in a database (Access, Microsoft Corp., Redmond, Wash.). The raw spectra (1024 points) were recorded as percentage reflectance. The spectra were processed in real−time by a 9−point running mean, and then the second difference (S˝) was calculated according to the formula

$$S''_n = S_{n-g} - 2 \times S_n + S_{n+g} \quad (1)$$

where S_n is the spectral value at point n, and g is the gap in data points. A g = 31 was used. The second difference was applied to reduce shifting baseline effects and isolate overlapping peaks. Then every fifth point was taken, resulting in a reduced second difference of 190 data points. Data analysis was performed on these reduced second difference spectra. The Principal Component Analysis (PCA) algorithm (Wold and Sjostrom, 1977) was implemented in the API data analysis module. The PCA method approximates the spectral vector of a poultry carcass with a linear combination of set uncorrelated (orthogonal) vectors:

$$Y \cong a_1 C_1 + a_2 C_2 + a_3 C_3 + ... + a_k C_k \quad (2)$$

where Y is the spectral vector, C_k is the kth factor (component), and a_k is the kth coefficient of the linear combination. Coefficients a_1 to a_k are called the scores of the spectral vector. In this way, the dimension of the spectra in a wavelength space can be transformed into a vector space with k dimensions spanned by the k factors. Using the PCA as preprocessor, multilayer perceptions (MLP) were available in the API software for classification of chicken carcasses. For the MLP classifier, the principal components were calculated from a sample data set. Each spectrum was approximated by a linear combination of these principal components. The scalar coefficients (scores) of this linear combination were then calculated for that sample. The scores were then used as inputs into the MLP. The MLP was pre−configured to one input layer, one layer of hidden nodes, and one output layer with two nodes. Learning algorithms, including the generalized delta−rule (Rumelhart et al., 1986) and Qprop (Fahlman, 1988), were applied to the MPL classifier.

After off−line development of the classification models, parameters (including weights and biases from the optimized neural network models) are saved and then incorporated into the on−line prediction module of the API software. In

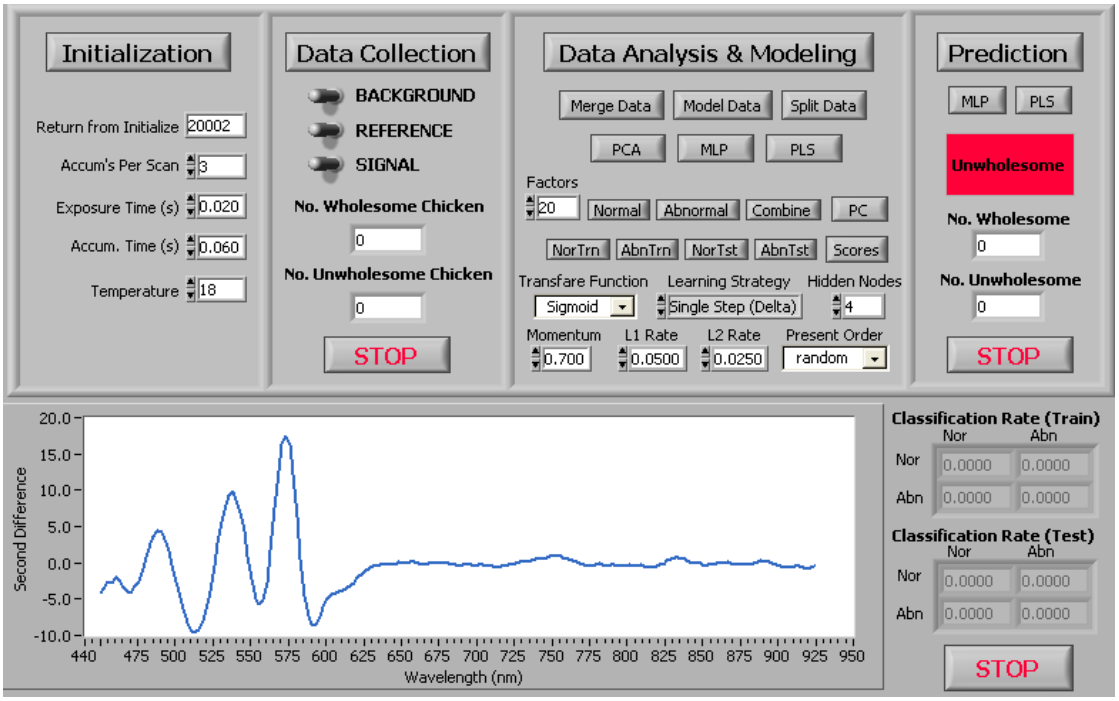

Figure 3. The Automatic Poultry Inspector (API) – main panel.

real−time operation, the prediction module can be used to immediately classify carcasses as wholesome or unwholesome from the spectral data acquired on−line.

PROCEDURES

Chicken carcasses were identified as wholesome or unwholesome by FSIS inspectors, placed onto portable hang−back racks by the inspectors' helpers, and collected on−site at a Conagra poultry processing plant in Athens, Georgia. The inspected chicken carcasses were immediately transported to a nearby room for spectral data acquisition. Chicken carcasses were manually hung on the shackles of a 17.7−m overhead conveyor running through a rectangular loop (6.7 × 3.1 m). The overhead conveyor was equipped with a variable frequency−controlled drive system. Line speeds at 140 and 180 birds/min were preset for this experiment. Before collecting spectra on chicken carcasses, reference and background measurements were taken. To establish a spectrally flat, repeatable, high−energy reference, a reference spectrum was collected by placing the fiber−optic probe 2 cm from a 14−mm thick piece of Spectralon reflectance target (Labsphere, Sutton, N.H.) of approximately 99% absolute reflectance throughout the wavelength region examined. A background measurement was taken, to compensate for the zero energy signal, by placing the optical probe 2 cm from the bottom of a black cylindrical Teflon™ sample cell with the light source turned off. Spectra were recorded as percent reflectance according to the formula:

$$\%\text{Reflectance} = \frac{100\times(\text{sample reflectance}-\text{background})}{(\text{reference}-\text{background})} \quad (3)$$

During spectra acquisition, the API data collection module was used to control the CCD detector, which was set at three accumulated scans with full vertical binning resulting in 1024 data points. The single−scan exposure time was 20 ms; consequently, a single chicken carcass was scanned over a total of 60 ms. A photoelectric sensor (Model QS30LDLQ, Banner Engineering Corp., Minneapolis, Minn.) was used to synchronize the data acquisition with bird position in the field of view. At 140 bpm, 900 wholesome and 852 unwholesome spectra were collected (two for each bird). Another 900 wholesome and 852 unwholesome spectra (two for each bird) were collected at 180 bpm. Afterward, the FSIS veterinary medical officer examined the wholesome or unwholesome condition of each bird, including specific postmortem conditions, and each diagnosis was recorded for correlation to the spectral database.

CLASSIFICATION MODELING

The raw spectra were recorded as percentage reflectance, 1024 points, 431.0 to 943.5 nm spaced 0.5009 nm apart. A 9−point running average and second difference with gap = 31 points was applied to each spectrum. Selection of every fifth point further reduced each spectrum to 190 points (450.6 to 924.0 nm).

The data was divided into three sets for the MLP classification method: training, test, and validation. The wholesome and unwholesome spectra sets were merged, in the order collected, to form one data set for each line speed. Every third spectrum, starting with the first, was used for training; every third spectrum, starting with the second, was used for testing; and every third spectrum, starting with the third, was used for validation. This division of data resulted in three separate datasets, each containing 300 wholesome and 284 unwholesome spectra. The principal components were calculated from the training set. Scores were then calculated for each spectrum in the training, testing, and validation sets. The numbers of input nodes to the MLP used for this study were 10, 20, and 30. The corresponding

numbers of hidden nodes were derived based on the square root of the input nodes, i.e. 3, 4, and 5, respectively.

The scores were then used as inputs into a feed−forward−back−propagation MLP. The output nodes were (0 1) or (1 0) depending on whether the sample was identified to be wholesome or unwholesome by the veterinarian. The MLP models were trained on scores from the training set. Scores from the test set were used to decide which network model and how much training was optimal. The validation set was then used to measure the performance of the model, independent of the training and testing datasets. Two learning strategies, delta and cumulative delta, and two transfer functions, tan h and sigmoid, (Rumelhart et al., 1986) were used for a total of four models for each training/validation/testing split of data.

RESULTS AND DISCUSSION

The average reflectance spectra of wholesome and unwholesome chicken samples are shown in figures 4a and 4b for line speed at 140 and 180 bpm, respectively. With the exception of baseline variations, the spectra of wholesome and unwholesome chickens were similar. The overall vertical offset of a particular spectrum was caused by variable scatter and surface reflectance, and small changes in distance to the sample, which have little to do with the category characteristics. To reduce visual impact of shifting baseline effects and isolate overlapping peaks, second differences (calculated with a gap size of 15.5 nm) were determined for all wholesome and unwholesome chicken samples. The mean second difference spectra were plotted for wholesome and unwholesome samples and are shown in figure 5a and 5b for line speed at 140 and 180 bpm, respectively. There were characteristic differences in absorption (peaks) and reflectance (valleys) between wholesome and unwholesome chickens. The most distinctive difference in absorption bands (peaks) among the wholesome and unwholesome samples occurred at 458, 490, 540, and 574 nm. The valleys occurred at 514, 556, and 592 nm and to a lesser extent at 716 and

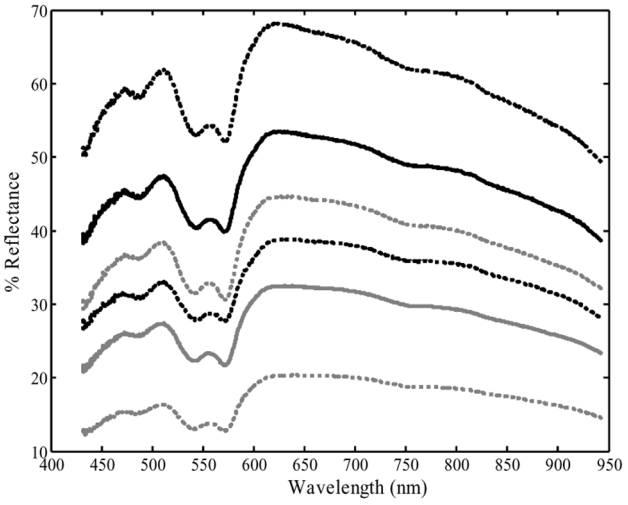

Figure 4a. Mean reflectance spectra (solid line) of wholesome (black) and unwholesome (gray) chicken carcasses, with one standard deviation envelope (dotted line) at 140 birds per minute.

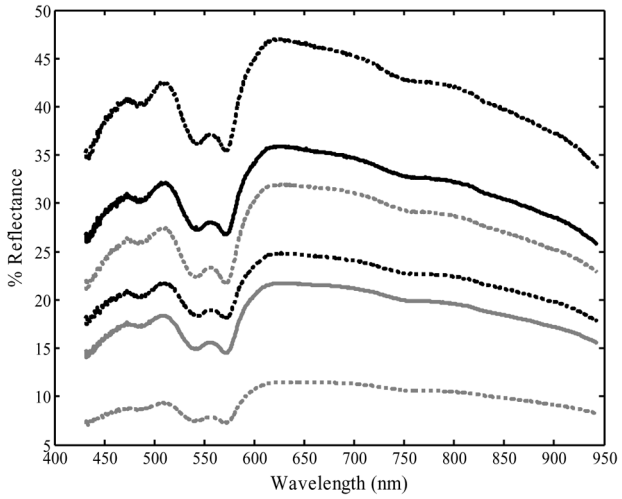

Figure 4b. Mean reflectance spectra (solid line) of wholesome (black) and unwholesome (gray) chicken carcasses, with one standard deviation envelope (dotted line) at 180 birds per minute.

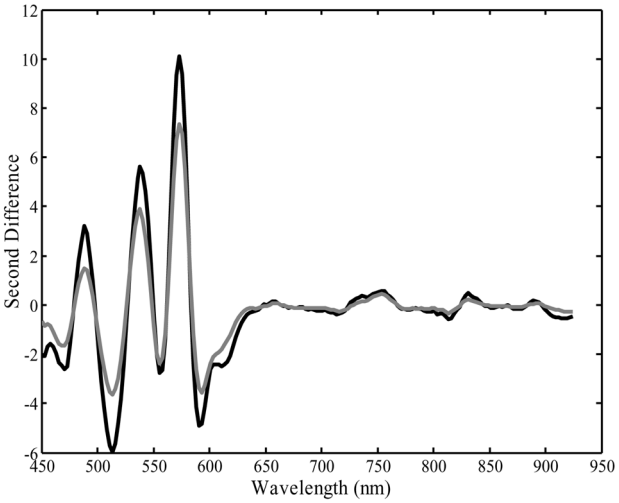

Figure 5a. Mean second difference spectra of wholesome (black) and unwholesome (gray) chicken carcasses at 140 birds per minute.

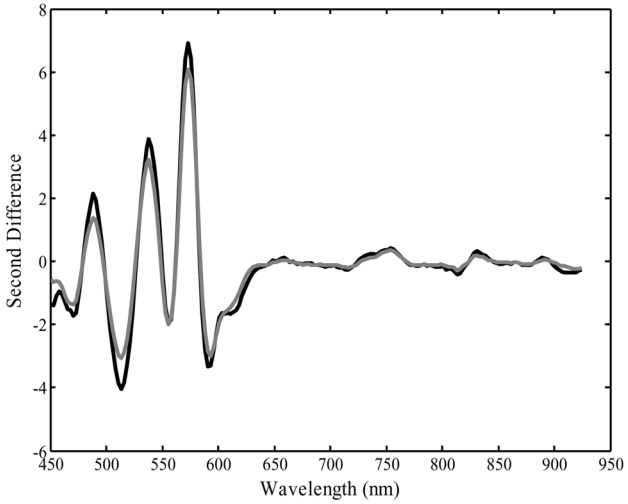

Figure 5b. Mean second difference spectra of wholesome (black) and unwholesome (gray) chicken carcasses at 180 birds per minute.

816 nm. Interestingly, at 740 and 835 nm, there were differences in absorption among the wholesome and unwholesome chicken carcasses.

For well−bled meat, the major pigment is determined at the meat surface by the relative amounts of three forms of myoglobin, i.e. deoxymyoglobin, metmyoglobin, and oxymyoglobin (Kinsman et al., 1994; Swatland, 1989). The deoxymyoglobin and oxymyoglobin components coexisted with metmyoglobin in both wholesome and unwholesome chicken meats and the three forms of myoglobin can inter−convert and may degrade through oxygeneration, oxidation, and reduction reactions when external processes such as cold storage, cooking, and irradiation are applied (Liu and Chen, 2000; Liu et al., 2003). The absorption bands around 458, 490, 540, and 574 nm represent the effects of various conformational structure of myoglobin, while the absorption bands at 740 and 835 nm could be a combination of lipids, water, and various forms of myoglobin absorptions. These absorption areas form a major base for spectral differentiation of wholesome chicken from unwholesome chicken.

PC 1 and PC 2 scores for the 140−bpm training set are plotted in figure 6. The PC 1 scores show wide variation for both wholesome and unwholesome samples. However, for the PC 2 scores, a pattern is evident in which the wholesome samples are positive and the unwholesome samples are negative, with some slight overlap. The loadings associated with PCs 1 and 2 are plotted in figures 7a and 7b. The loading weights, being regression coefficients at specific wavelengths for a PC, show the relative contribution of those wavelengths to the amount of spectral variance for which that PC accounts. Thus a large positive or large negative weight indicates a significant contribution for the corresponding wavelength. The loading shapes of both PC 1 and PC 2 are similar to that of the second difference spectra, but the wavelength region at 490 nm is much more prominent in PC 2 than in PC 1. Metmyoglobin has been correlated to this region (490 nm), while oxymyoglobin has been correlated to the regions of 545 and 560 nm (Liu et al., 2000) that are also evident in PC 2. Liu et al. (2000) found more variation in metmyoglobin for diseased chicken meat, concluding it to be a degraded form of both oxymyoglobin and deoxymyoglobin.

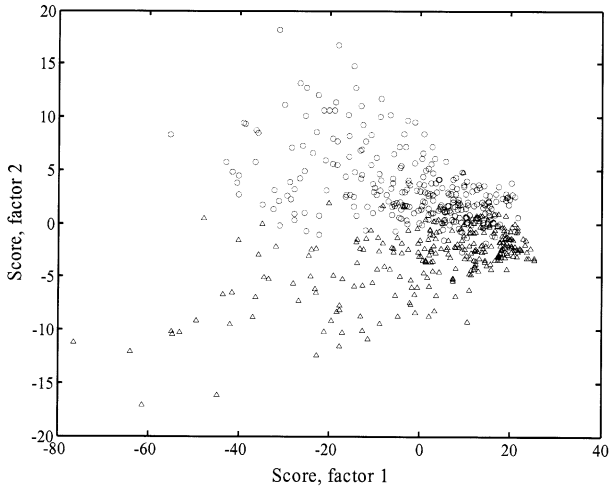

Figure 6. PCA score plot of components 1 and 2 for wholesome (circle) and unwholesome (triangle) chicken carcasses.

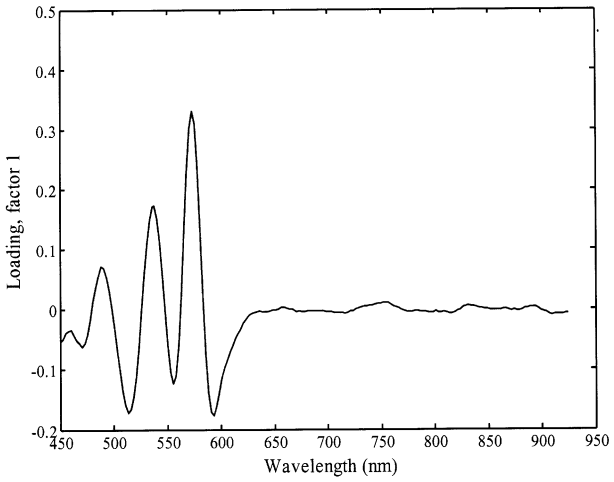

Figure 7a. The first principal component, determined from principal component analysis on training set data.

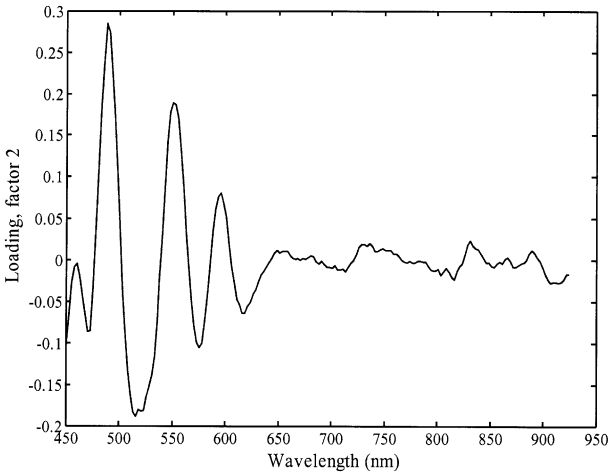

Figure 7b. The second principal component, determined from principal component analysis on training set data.

Figure 8 shows the Root Mean Square Error of Cross−Validation (RMSECV) for the 140−bpm training data set. With one−sample−out cross−validation, the error continued to decrease with each additional PC. Although the last significant incremental decrease in error occurs with PC 5, additional PCs do not appear to describe noise variance and result in further, though slight, error reductions. The 180−bpm training data set showed similar results.

Two back−propagation rules (delta and cumulative delta) and two transfer functions (sigmoid and tanh) were used for a total of four models (table 1) for each training/test/validation split of data. As expected, results from the training data used for the neural network learning process at both 140 and 180 bpm were generally high, around 97%. For 10−, 20−, and 30−input MLP, testing set and validation set results for each of the four models, using spectral data acquired at 140 bpm, are shown in table 2. Using as inputs the scores calculated from 10 PCs, the overall classification accuracies ranged from 83% to 90%. With 20 input nodes, the classification accuracies improved, with Model 1 achieving the best accuracies. For the test data set, 96% of wholesome carcasses

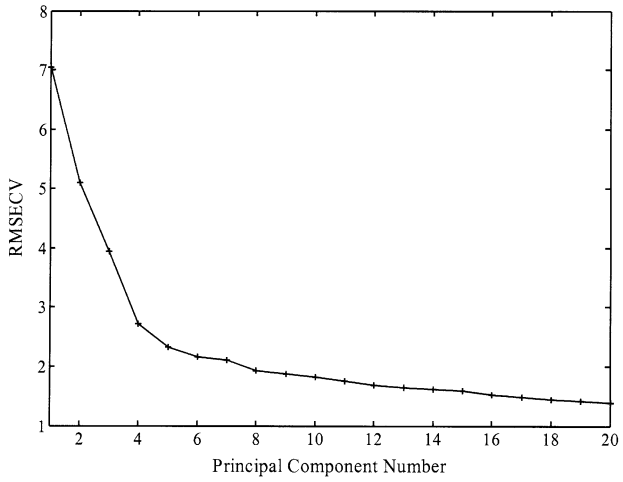

Figure 8. Cross−validation RMSECV curve for training set data.

and 92% of unwholesome carcasses were correctly classified, for an average of 94%. For the validation set, 95% of wholesome and 92% of unwholesome carcasses were correctly classified, for an average of 93.5%. With 30 input nodes, the classification accuracies did not increase significantly. In general, the models using the delta−learning rule performed better than those using the cumulative delta−learning rule. It was also noted that the classification accuracies of Model 4, using the cumulative delta learning rule with the hyperbolic tangent transfer function, was consistently lower than those of the other three models.

Table 3 shows the testing set and validation set results for the models using spectral data acquired at 180 bpm. The classification accuracies of the four models ranged from 81% to 88% when using 10 input nodes, and increased for 20 and 30 nodes. With 30 input nodes, Model 1 using the delta learning rule and sigmoid transfer function achieved the highest classification accuracy, correctly classifying 95% wholesome and 92% unwholesome carcasses in the test set, and 94% wholesome and 92% unwholesome in the validation set.

In general, disease conditions in chickens are often evidenced by changes in skin color and the tissue composition that are detectable through visible and near−infrared spectroscopy. A real−time inspection system must have the capacity for rapid spectral measurement, data processing, and classification computation within a limited time window. In addition, poultry inspection can present a dynamic situation as populations of chickens may vary between different breeds, seasons, or dietary regimens. The results of this study show that a Vis/NIR inspection system can successfully operate at high speeds to classify wholesome and unwholesome birds. Also, the use of MLP for classification provides the potential for adaptive inspection to handle changing poultry populations. Creating such automated calibration models that can be updated online will be tested in future studies.

Table 1. Neural network models.

Model	Learning Rule	Transfer Function
1	Delta	Sigmoid
2	Delta	Tanh
3	Cumulative Delta	Sigmoid
4	Cumulative Delta	Tanh

Table 2. Classification accuracy at 140 bpm for the 10, 20, 30 input nodes to the MLP.

	Wholesome Carcasses	Unwholesome Carcasses	All Carcasses	
10 input nodes				
Model 1	92	88	90	Test
	90	89	89.5	Validation
Model 2	91	88	89.5	Test
	91	87	89	Validation
Model 3	90	88	89	Test
	89	84	86.5	Validation
Model 4	91	78	84.5	Test
	90	76	83	Validation
20 input nodes				
Model 1	96	92	94	Test
	95	92	93.5	Validation
Model 2	95	92	93.5	Test
	94	92	93	Validation
Model 3	93	92	92.5	Test
	94	91	92.5	Validation
Model 4	93	90	91.5	Test
	91	89	90	Validation
30 input nodes				
Model 1	95	93	94	Test
	94	92	93	Validation
Model 2	95	92	93.5	Test
	95	91	93	Validation
Model 3	94	92	93	Test
	93	92	92.5	Validation
Model 4	90	90	90	Test
	91	90	90.5	Validation

Table 3. Classification accuracy at 180 bpm for the 10, 20, 30 input nodes to the MLP.

	Wholesome Carcasses	Unwholesome Carcasses	All Carcasses	
10 input nodes				
Model 1	87	86	86.5	Test
	89	87	88.5	Validation
Model 2	87	82	84.5	Test
	86	85	85.5	Validation
Model 3	84	88	86	Test
	82	80	81.5	Validation
Model 4	78	84	81	Test
	80	82	81.5	Validation
20 input nodes				
Model 1	94	91	92.5	Test
	92	90	91.5	Validation
Model 2	93	92	92.5	Test
	91	92	91.5	Validation
Model 3	90	92	91	Test
	90	91	90.5	Validation
Model 4	92	90	91	Test
	91	90	90.5	Validation
30 input nodes				
Model 1	95	92	93.5	Test
	94	92	93	Validation
Model 2	93	92	92.5	Test
	95	90	92.5	Validation
Model 3	91	92	91.5	Test
	90	91	90.5	Validation
Model 4	91	90	90.5	Test
	90	90	90	Validation

CONCLUSIONS

A new Vis/NIR spectroscopic system was developed using modularized software components and was able to collect

real−time spectral measurements for chickens running on high−speed processing lines. Data analysis and modeling demonstrated that the system can successfully differentiate between wholesome and unwholesome birds. At 140 bpm, Model 1 (using 20 input nodes to the MLP) was able to correctly classify 95% and 92% of wholesome and unwholesome birds, respectively. At 180 bpm, Model 1 (using 30 input nodes to the MLP) was able to correctly classify 94% and 92% of wholesome and unwholesome birds, respectively. The Automated Poultry Inspector program also has a module for real−time prediction and the capacity to accommodate other functions as needed for real−time operation. The results of this study show this automated poultry inspection system based on Vis/NIR spectroscopy is ready for implementation on commercial high−speed poultry processing lines for real−time operation. Using such an automated inspection system would greatly improve overall production efficiency of processing plants.

REFERENCES

Chao, K., Y. R. Chen, W. R. Hruschka, and F. B. Gwozdz. 2002. On−line inspection of poultry carcasses by a dual−camera system. *J. Food Eng.* 51(3): 185−192.

Chen, Y. R., and D. R. Massie. 1993. Visible/near infrared reflectance and interactance spectroscopy for detection of abnormal poultry carcasses. *Transactions of the ASAE* 36(3): 863−889.

Chen, Y. R., R. W. Huffman, B. Park, and M. Nguyen. 1996. Transportable spectrophotometer system for on−line classification of poultry carcasses. *Appl. Spectr.* 50(7): 910−916.

Chen, Y. R., W. R. Hruschka, and H. Early. 2000. A chicken carcass inspection system using visible/near−infrared reflectance: in plant trials. *J. Food Process Eng.*23(2): 89−99.

Daley W., R. Carey, and C. Thompson. 1994. Real−time color grading and defect detection of food products. *Optics in Agriculture, Forestry, and Biological Processing. SPIE* 2345: 403−411.

Fahlman, S. E. 1988. An empirical study of learning speed in back propagation networks. In *Proc. 1988 Connectionist Models Summer School*, eds. T. J. Sejnowski, G. E. Hinton, and D. S. Touretzky, 38−51. San Mateo, Calif.: Morgan Kaufmann.

Kinsman, D. M., A. W. Kotula, and B. C. Breidenstein. 1994. *Muscle Foods*, 71−74. New York: Chapman and Hall.

Lawrence, K. C., B. Park, D. P. Smith, W. R. Windham, and P. Feldner. 2002. Hyperspectral system calibration for improved contaminant detection on poultry carcasses. ASAE Paper No. 023063. St. Joseph, Mich.: ASAE.

Liu, Y., Y. R. Chen, and Y. Ozaki. 2000. Characterization of visible spectral intensity variations of wholesome and unwholesome chicken meats with two−dimensional correlation spectroscopy. *Appl. Spectr.* 54(4): 587−594

Liu, Y., and Y. R. Chen. 2000. Two−dimensional correlation spectroscopy study of visible and near−infrared spectral variations of chicken meats in cold storage. *Appl. Spectr.* 54(10): 1458−1470.

Liu, Y., X. Fan, Y.R. Chen, and D.W. Thayer. 2003. Changes in structure and color characteristics of irradiated chicken breasts as a function of dosage and storage time. *Meat Science.* 63(3): 301−307.

Park, B., Y.R. Chen, M. Nguyen, and H. Hwang. 1996. Characterizing multispectral images of tumorous, bruised, skin−torn, and wholesome poultry carcasses. *Transactions of the ASAE* 39(5): 1933−1941.

Rumelhart, D. E., G. E. Hinton, and R. J. Williams. 1986. Learning internal representations by error propagation. In *Parallel Distributed Processing*, Vol. 1: Foundations, eds. D. E. Rumelhart, J. L. McClelland, and the PDP Research Group, 318−363. Cambridge, Mass.: MIT Press.

Swatland, H. J. 1989. A review of meat spectrophotometry (300 to 800 nm*). Can. Inst. Food Sci. Technol. J.* 22: 390−402.

USDA. 1984. A review of the slaughter regulations under the Poultry Products Inspection Act. Regulations Office, Policy and Program Planning, FSIS, USDA, Washington, D.C.

USDA. 1998. HACCP−Based inspection models project: Diseases and conditions observable in meat and poultry. FSIS, USDA, Washington, D.C. http://www.fsis.usda.gov/OA/haccp/foscp.htm. Accessed: 19 February 2004.

Wold, S., and M. Sjostrom. 1977. *Chemometrics: Theory and Application*, ed. B. R. Kowalski, 242−282. Washington, D.C.: American Chemical Society.